Transportation Research Part D 114 (2023) 103548

Contents lists available at ScienceDirect

Transportation Research Part D

journal homepage: www.elsevier.com/locate/trd

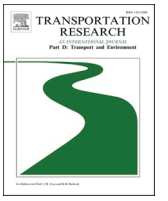

Repurposing mesoscale traffic models for insights into traveler heat exposure

Rui Li [a,*], Mikhail V. Chester [a,b,c,e], David M. Hondula [d,e], Ariane Middel [d,e,f], Jennifer K. Vanos [c], Lance Watkins [d]

[a] School of Sustainable Engineering and Built Environment, Arizona State University, Tempe, AZ 85287, USA
[b] Metis Center for Infrastructure and Sustainable Engineering, Arizona State University, Tempe, AZ 85287, USA
[c] School of Sustainability, Arizona State University, Tempe, AZ 82581, USA
[d] School of Geographical Sciences and Urban Planning, Tempe, AZ 85281, USA
[e] Global Institute of Sustainability and Innovation, Arizona State University, Tempe, AZ 85281, USA
[f] School of Arts, Media and Engineering and School of Computing, Informatics, and Decision Systems Engineering, Arizona State University, Tempe, AZ 85281, USA

ARTICLE INFO

Keywords:
Urban
Climate
Active transportation
Personal heat exposure

ABSTRACT

Climate change is poised to significantly increase people's heat exposure, yet there remain limited insights into how individuals experience heat in the conjunction of behavior and infrastructure. We developed a simulation platform - Icarus - to estimate traveler's heat exposure at both personal and population scales at the interface of travel behavior, microclimate, and the built environment. Icarus is applied to the Phoenix metropolitan region as a case study using three different temperature measurements: air temperature (T_{air}), mean radiant temperature (T_{MRT}), and wet bulb globe temperature (T_{WBGT}). The case study analysis shows that travel patterns (such as trip duration and the trip start time) for different demographic groups affect personal and population heat exposure. Different temperature measures also resulted in widely varying estimates of personal heat exposure.

1. Introduction

Climate change and rapid urbanization pose heat-related health challenges for urban residents, especially in the transportation sector. Automobile dependence contributes to urban heat island effects in cities, including large surface areas that store heat as well as vehicle waste heat (Hoehne et al., 2020; Kamruzzaman et al., 2018; Kolbe, 2019). Reducing dependence on cars has been proven to create environmental and health benefits, such as reducing GHG emissions (de Nazelle et al., 2010), mitigating city congestion (FlLOW Project, 2016), and lowering the amount of urban area dedicated to paved parking and road infrastructures. Increasing non-vehicle trips can improve physical health (Hamer & Chida, 2008). Despite the positive outcomes of active travel there are concerns that the combined effect of increasing urban heat and climate change will contribute to adverse health outcomes for outdoor travelers (Eisenman et al., 2016; Hondula et al., 2014). Many heat-related health risks disproportionately impact populations with low socioeconomic status (Karner et al., 2015). Cities have carried out heat exposure mitigation initiatives, such as planning for cooling shelters or increasing shading along sidewalks, to combat the increasing heat-related illness and discomfort among residents (City of Mesa, 2014; Phoenix, 2021). Rapid advancements into individual heat exposure offer significant opportunity to focus mitigation

* Corresponding author.

https://doi.org/10.1016/j.trd.2022.103548
Received 15 May 2022; Received in revised form 21 October 2022; Accepted 24 November 2022

strategies.

Heat exposure studies have provided insights into the relationship between high temperature and adverse health outcomes typically at the population scale (e.g., Bao et al., 2015; Hondula & Davis, 2012; Reid et al., 2009). Studies have examined how heat-caused adverse health outcomes are associated with specific demographic features (Chow et al., 2012; Karner et al., 2015). The population-scale "heat" exposure studies are often limited to proxy variables like the highest land surface air temperature (T_{air}) (Bao et al., 2015; Bernhard et al., 2015; Kuras et al., 2017). However, they do not recognize the total spatiotemporal variation of the individual's heat load or travel behavior that significantly impacts personal exposure. Personal heat exposure studies, which have used portable devises to measure the temperature as people, provide a more precise understanding of individual experience with heat in heterogeneous city environments (Glass et al., 2015; Kuras et al., 2015; Kuras et al., 2017). However, they are often limited to small sample sizes and short measurement periods and are challenging to generate population-scale heat exposure findings. New opportunities are emerging to assess individual exposure.

The advancements of mesoscale travel models and ambient temperature simulations provide unique opportunities to advance personal heat exposure research methods within heterogeneous city environments across a population. Mesoscale travel models, such as the activity-based model (ABM), provide daily human activity and travel patterns (Pendyala et al., 1997). The ABM is a state-of-the-art simulation used by metro regions to estimate travel characteristics of individuals and households for long-term planning. ABMs have been used to study personal air pollution exposure and heat exposure at the location of activities (Karner et al., 2015; Yoo et al., 2015). However, neither the specific travel pattern (path) nor the ambient temperature variability along the transportation infrastructure were considered in their study. Furthermore, novel temperature metrics provide new opportunities for assessing heat exposure not simply as air temperature (Hondula et al., 2021). While air temperature can be insightful, perhaps more useful is the net radiation that a traveler is exposed to (Middel et al. 2017).

Towards creating novel methods and insights into individual heat exposure across entire urban populations, we use state-of-the-art mesoscale travel simulations and fine-scale microclimate data to develop a simulation platform for urban environments. The simulation platform—Icarus—joins the ABM travel behavior output with temperature data, parcel characteristics, household characteristics, and travel characteristics. We first introduce the Icarus structure, the datasets used, parsing and assumptions. Next, the simulation and heat exposure calculations are described. Lastly, Icarus is applied to the Phoenix metropolitan region as a case study. Metro Phoenix is a particularly appropriate case given summertime extreme heat, and rapid urbanization with population increase. Further, climate change is expected to increase the extreme heat in both intensity and duration (Pörtner et al., 2022)—thus, Metro

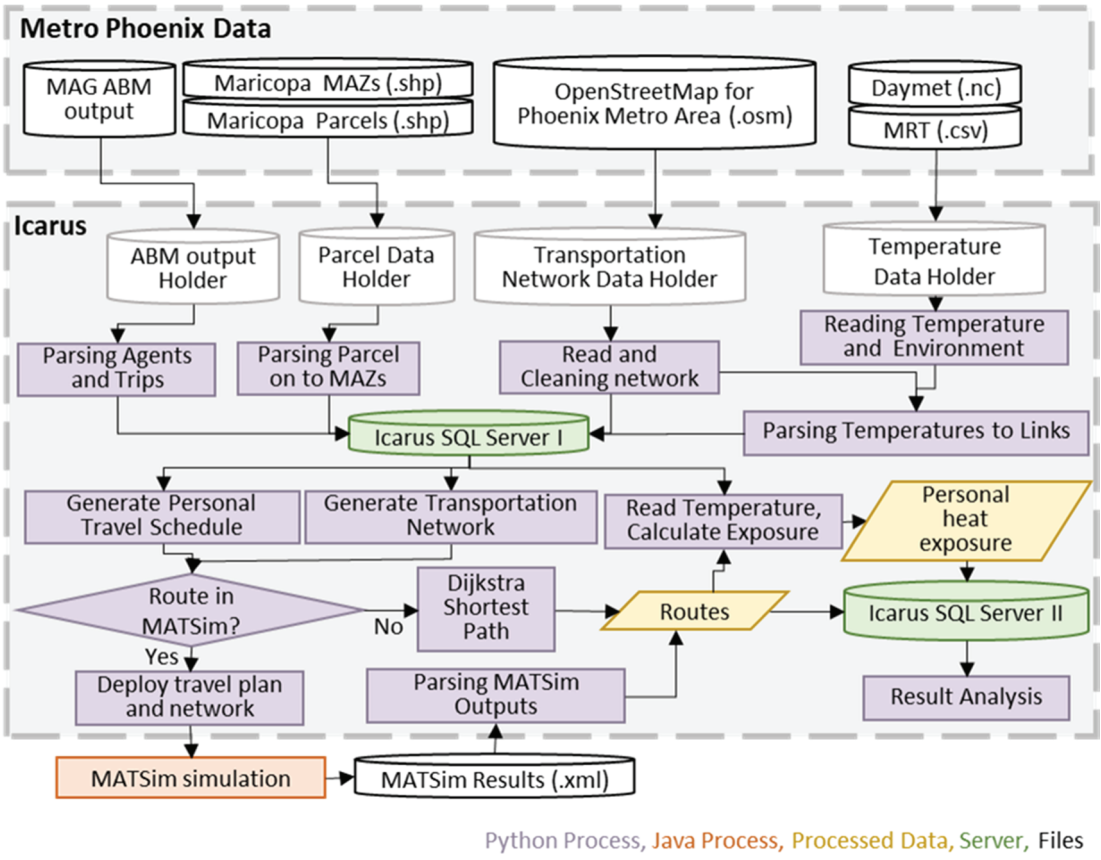

Fig. 1. Icarus Framework.

Phoenix is a harbinger of the future for other cities. Findings from this study can guide urban planning, public health policymaking, and heat stress mitigation strategies.

2. Methods

The structure of Icarus consists of two core processes: data ingestion and simulation. Fig. 1 illustrates the major processes and the key datasets used. During data ingestion, Icarus ingests critical datasets such as infrastructure networks, the ABM, and environmental temperature data (Icarus SQL Server I in Fig. 1). From this database, Icarus builds a transportation network with spatiotemporal temperature information, and population group with travel schedules to start the simulation. The simulation platform estimates personal travel patterns and heat exposure based on agents' daily travel schedules. A second database (Icarus SQL Server II in Fig. 1) stores the simulation results for further analysis, such as estimating the population subgroups and the locations with high heat stress. The following section explains the modeling details, data parsing techniques, heat exposure calculations, and hot trip identification.

2.1. Icarus

Icarus is a personal heat exposure simulation module developed with Python and intended for transportation planning, urban planning, and policy research use. Agents with complementary information (e.g., age, gender, travel, and activity pattern) are primary simulation objects. Icarus estimates personal heat exposure by routing agents in the city and tracing the environmental temperature one experiences during daily trips and activities. Icarus needs multiple datasets to achieve the functions and has essential modules to parse the input data in different formats into the same simulation environment.

2.1.1. Core data ingestion

Parsing and unifying urban-related data sources is a critical first step. The core datasets ingested are described in Table 1 and detailed in the following subsections. Data requirements include the ABM, parcel data, transportation network data, temperature profiles, and environmental data. The ABM and parcel data are used to extract travel schedules and locations. Transportation networks and fine-scale temperature metrics are needed to route the trips and estimate heat exposure of travelers. Towards improving the scalability of Icarus, publicly available datasets are retrieved from the OpenStreetMap (for the transportation network) (OpenStreetMap Contributors, 2015) and National Oceanic and Atmospheric Administration (for T_{air}) (Oak Ridge National Laboratory, 2020). The following sections explain the details of each dataset and data parsing techniques.

2.1.1.1. Activity-based model (ABM) and land parcel data. The ABM and land parcel data are core inputs to Icarus towards estimating fine-scale movements of individuals. Metropolitan Planning Organizations, such as the Maricopa Association of Governments (MAG) in Arizona, use travel surveys and complementary datasets to generate ABMs. ABMs contain a synthetic population that captures individual actor characteristics, such as their education, age, gender, and job type. ABMs also included daily travel plans, including individual and group travel behavior within households. The trips in the ABM have precise origins and destinations (described through either Traffic or Micro Analysis Zones, TAZ and MAZ), travel modes, travel times, trip durations, trip purposes, and the person who carried out the trip. Icarus follows the individual and group travel defined in the ABM when loading the data into the simulation environment. For instance, very young travelers and the school-age population often travel with at least one older member in the household. Icarus parses the group travelers and their trips by assigning them the exact origin and destination and the same start and end trip time. However, Icarus considers these grouped travels as several separate trips in the routing and exposure estimation process.

Icarus relies on land parcel data to refine the precise locations of trip origins and destinations. Icarus needs the exact origin and destinations (O/D), such as a building or parcel, to initiate the routing and assess environmental exposure profiles. However, a MAZ or TAZ contains dozens to hundreds of parcels. Icarus depends on county assessor databases – publicly available land parcel datasets that describe the property and building locations – to downscale the O/D for each trip from MAZ or TAZ to a specific spot. The traffic analysis zones are spatially joined with fine-scale assessor data to identify the parcels inside each transportation zone. Icarus then assigns the parcel's location to the MAZ or TAZ O/D randomly. The Land Parcel data is also used to estimate if an air-conditioner (AC) is present during the activity.

2.1.1.2. Roadway network. The trip routing process requires roadway inputs, especially the biking/walking network. The roadway network data is sourced from OpenStreetMap (OpenStreetMap Contributors, 2015). OSM contains rich information about the roadway

Table 1
Core input data, format, and source for this project.

Data name	Data format	Data Source
Activity-based model output (ABM)	.csv,.db	City or regional planning organization
Land Parcel data	.shapefile, or.csv file with locations	City or county assessor database
Transportation network data	.osm or.shp	OpenStreetMap or Tiger shapefile
Temperature data	.net4,.csv, or raster file with location information	National Oceanic and Atmospheric Administration or regional estimation

network for active trips, including length and allowed travel mode. In the data loading process, Icarus uses the Python module Osmium to read the OSM as arcs (links) and vertices (nodes). Considering the agility of walking and biking trips, the single-direction arcs which overlap with each other but have the same end nodes are simplified as one bidirectional arc. Additional nodes are added at the intersection of arcs if Icarus finds absent points at the crossings. The loaded network is stored as a Networkx Graph (Hagberg et al., 2008) in the simulation environment, and allows for walking and biking routing.

2.1.1.3. Temperature metrics. Icarus provides flexibility to incorporate different types of environmental temperatures. Considering air temperature, radiation, humidity, and wind effects on personal comfort, T_{air}, T_{MRT}, and T_{WBGT} are each introduced.

T_{air} measures how hot/cold the air is without considering other effects such as wind, radiance, and humidity effects. T_{air} is obtained from the Daymet dataset, which describes the daily temperature lows and highs in 1 km by 1 km grids, available from 1980 over continental North America (Thornton et al., 2021). Assuming the minimum temperature (T_{min}) occurs before dawn (t_{dawn}), the maximum temperature (T_{max}) occurs in the early afternoon (t_{peak}). The hourly air temperature function can be interpolated using a sinusoidal function as in Eq. (1):

$$T_{air,\,t} = \begin{cases} \left(\frac{T_{max}+T_{min}}{2}\right) - \left(\frac{T_{max}-T_{min}}{2}\right)*\cos\left(\pi*\frac{t_{dawn}-t}{24+t_{dawn}-t_{peak}}\right), \; if t < t_{dawn} \\ \left(\frac{T_{max}+T_{min}}{2}\right) - \left(\frac{T_{max}-T_{min}}{2}\right)*\cos\left(\pi*\frac{t_{peak}-t}{t_{peak}-t_{dawn}}\right), if t_{dawn} \le t < t_{peak} \\ \left(\frac{T_{max}+T_{min}}{2}\right) - \left(\frac{T_{max}-T_{min}}{2}\right)*\cos\left(\pi*\frac{24+t_{dawn}-t}{24+t_{dawn}-t_{peak}}\right), \; if \; t \ge t_{peak} \end{cases} \quad (1)$$

Emerging mean radiant temperature (T_{MRT}) data provide opportunities to examine the net radiation experienced during trips. T_{MRT} measures the environmental radiation on the object, from the sun and reflected from surfaces (Aminipouri et al., 2019; Middel et al., 2017). T_{MRT} is commonly addressed as a better substitute for T_{air} but was difficult to obtain from observation. New advanced approaches exist to generate T_{MRT} from deep learning Google Street View images by detecting the sky, buildings, trees, pavements, and shadings (Middel et al., 2017).The ABM model and simulated T_{MRT} can be used in personal heat exposure studies.

T_{WBGT} is a widely used index of heat stress that includes humidity, solar radiation, sun angle, and wind in addition to air temperature (Budd, 2008; OSHA, 2015). T_{WBGT} is acquired from either measurements (Budd, 2008) or estimation using empirically developed models (OSHA, 2015; Stull, 2011; Vanos et al., 2021). As citywide T_{WBGT} is less common, Icarus uses functions from OSHA (2015), Vanos et al. (2021) and Stull (2011) to calculate T_{WBGT} when both T_{air} and T_{MRT} are presented. The OSHA (2015) manual offers Eqs. (2) and (3) for T_{WBGT}:

$$T_{WBGT} = 0.7*T_W + 0.2*T_G + 0.1*T_{air} \quad (2)$$

where T_w is the Nature Wet-Bulb Temperature, and T_G is the Globe Temperature. Icarus adapts the T_w calculation from Stull (2011) showing in Eq. (3):

$$T_w = T_{air}atan[(RH+8.314)^{0.5}] + atan(T_{air}+RH) - atan(RH-1.676) + 0.004(RH)^{1.5}atan(0.0231RH) - 4.686 \quad (3)$$

where RH is the relative humidity.

For indoor, or outdoor environments without solar load, T_G equals to T_{air}. For an outdoor environment with solar load, T_G in Eqs. (2) and (3) is calculated by solving for T_G in the formula Eq. (4) from Vanos et al.(2021):

$$T_{MRT} = \sqrt[4]{(T_G+273.15)^4 + (0.24+2.08v_a^{0.5}+1.14v_a^{0.667})(T_G-T_{air})*10^8} - 273.15$$

Where v_a is the wind velocity.

The ingested temperature and environmental data can be in different formats, spatial resolutions, and temporal resolutions. Using Eq. (1) Icarus interpolates the min and max T_{air} to the exact temporal resolution as T_{MRT}. Icarus first builds a transportation network with spatiotemporal T_{air} and T_{MRT} information by retrieving the average temperature value in a 30-meter buffer radius around the network links. The T_{WBGT} on each link is then calculated using T_{air} and T_{MRT} values.

2.1.2. Simulation

After the core data ingestion, Icarus simulates agent behavior by extracting the trip and activity schedules from the ABM output, assigning the location of activities and O/D of trips to the parcels, then routing the trips on the roadway network. The personal heat exposure is then calculated using the trip path and activity locations. The following sections discuss the details and assumptions of each step in the simulation process.

2.1.2.1. Routing active trips. Icarus can accommodate two simulation engines: a Dijkstra shortest pathfinder or a MatSIM travel simulation. The Dijkstra shortest path algorithm finds the route for each trip in a distance or temperature-weighted roadway network. It returns the shortest path between the origin–destination (OD) pair with a distance-weighted network. With distance-temperature-weighted networks, Icarus selects lower temperatures but slightly longer routes if such paths exist. Routes of in-vehicle trips would not affect the temperature measures that an agent experiences as they are constantly under AC. Hence, the model does not route personal

car and public transport trips. MatSIM is the start-of-art open-source agent-based simulation platform for transportation planning. Icarus can generate the transportation network, agent plans, and the simulation configuration file required by MatSIM. While computationally equivalent to Dijkstra, MatSIM can be used to adjust travel schedules with modifications to the underlying utility function. This paper uses Dijkstra's shortest pathfinder for the proof-of-concept case study.

2.1.2.2. Heat exposure calculation. The activities and trips can occur both outdoors and in climate-controlled environments. In studying heat exposure Icarus assumes that agents taking in-vehicle trips or having activities in the AC-cooled parcels have significant heat reprieve. In contrast, biking and walking trips that occur outdoor or activities on parcels without AC are assumed to be carried out with no temperature control and under constant heat stress. Whether a parcel has AC or not is determined by the Land Parcel data, explained in detail in the case study session.

Heat exposure measures estimate the given environmental temperature trips and activities are likely to experience. Icarus sets the default T_{air} in an AC-cooled environment as 26.6 °C (80 °F). As such, for in-vehicle trips and activities under AC, their T_{air} exposure is constantly 26.6 °C (80 °F), and the T_{MRT} exposure would be equal to T_{air} under indoor environment (Kántor & Unger, 2011). Heat exposure for active trips under outdoor environment is calculated in Eq. (5):

$$T_{i,j} = \frac{\sum_{r \in R}(L_r * T_r)}{\sum_{r \in R} L_r} \tag{5}$$

where $T_{i,j}$ is the ambient temperature for a person i in trip j. $T_{i,j}$ can be either T_{air}, T_{MRT}, or T_{WBGT}. R is the collection of links on the route for a trip j. Link r should always be in R. T_r is the temperature (T_{air}, T_{MRT}, or T_{WBGT}) at the link r when trip j happens. L_r is the length of link r. The calculated trip and activity heat exposure can then be used for heat stress classification.

2.1.3. Heat stress classification

Icarus provides three heat stress classification matrices to rank the active trips heat exposure level, recognizing the variety of temperature measures available. The in-vehicle trip's heat exposure is not classified as they are assumed to have AC. The WBGT work/rest table is introduced to rank the trip heat exposure using T_{WBGT} and trip duration. A four-level rating scheme based on the quartile of calculated T_{MRT} and T_{air} for the simulated agents is used to rank the trip heat exposure from *cool* to *very hot*. We introduce the *Flow Ratio* to identify the locations where trips with the top level of heat stress take place.

Icarus introduces the WBGT work/rest table (W/R table), widely used in the industry to guide worker work and rest duration (ACGIH, 2019; Epstein and Moran, 2006; Sutherland, 2015), to assess travelers heat stress under T_{WBGT} exposure. The W/R table suggests the work and rest cycles a person should follow under different environmental temperatures, considering their time in that environment, the clothing they wear, their workload, and acclimation to heat (ACGIH, 2019; Iverson et al., 2020). Icarus adapts the W/R table (Sutherland, 2015) by assuming that active travel is the working status, while the activities after the trip are at resting status. Walking and biking are classified as moderate and heavy workloads according to their metabolic equivalent of task level (National Cancer Institute, 2002; Tudor-Locke et al., 2009). Assuming all agents in the ABM output are acclimated, Table 2 shows the adjusted W/R table. Based on duration and T_{WBGT} the heat stress levels of trips include *no risk*, *low risk*, *moderate risk*, *high risk*, and *extreme risk* (Table 2). Besides the listed stress levels, Icarus introduces a *violation of the W/B* level to categorize the trips that exceed the suggested work/rest cycle.

There is no standard threshold to distinguish low to high heat exposure using T_{MRT} and T_{air}. Hence, the heat stress level of these temperature metrics are grouped based on the trip's T_{MRT} and T_{air} quartiles. From the low to high temperature, trips are grouped as *cool* (lowest 25 %), *warm* (25–50 %), *hot* (50–75 %), and *very hot* (highest 25 %).

The *Flow Ratio* is defined as the proportion of the traffic flow contributed by trips with the top heat stress level and is calculated as per Eq. (6):

$$FlowRatio = \frac{F_T}{F_{All}} \tag{6}$$

The link flow counts the number of trips passing through the one-meter length of roadway in the simulation day. In Eq. (6), F_T is the link flow of very hot trips or trips that violate the WBGT W/R tables. F_T refers to the link flow of all trips. The *Flow Ratio* ranges between 0 and 100 %. A *Flow Ratio* greater than 50 % is alarming, as over half of the trip crossing is through roadway sections that are under top heat stress. Demonstrating the Flow Ratio in the network could help to identify the locations of trips with high heat stress.

Table 2
WBGT Work/rest Table Adapted from Sutherland (2015).

risk level	T_{WBGT}		trip/activity duration (minutes)	
	(C°)	(F°)	Walking (moderate work)	Biking (heavy work)
no risk	25.6–25.9	78–79.9	Continuous	50/10
low	26–28.9	80–84.9	50/10	40/20
moderate	29–30.9	85–87.9	40/20	30/30
high	31–31.9	88–90	30/30	20/40
extreme	>32	>90	20/40	10/50

2.1.4. Heat reprieve as AC

Activities carried out in an AC-cooled environment allow agents who travel under excessive heat to get reprieve and restore their body temperature. Trips from the ABM are in two general categories: in-vehicle trips and active trips which were assumed to happen outdoor. To determine the portion of travelers that cannot get heat reprieve Icarus categorizes the trips and their reprieve conditions based on Fig. 2. In-vehicle trips are assumed constantly under AC. If active trips end at locations with AC, agents can get reprieve. On the contrary, agents may not be reprieved if they stop at locations without AC or stay in the AC-cooled environment for a short duration. Icarus determines whether an active outdoor trip can relieve excessive heat exposure by considering the trip destination, AC conditions, and the duration agents stay in the cooled environment. Eq. (7) is used to determine cumulative heat exposure for trips and activities following:

$$E_i = -t_{act,i} * 26.6^{\circ}C + t_{trip,i} * T_{trip,i} \tag{7}$$

where $t_{act,i}$ and $t_{trip,i}$ are the duration of activity and trip, $T_{trip,i}$ is the air temperature of the trip. If E_i is greater than 0, then the time an agent stays in the AC-cooled room is long enough to get a reprieve. Otherwise, the trip cannot get reprieved indoors since the time one stays in the AC is too short.

2.2. Metro phoenix case study

The implementation and testing of Icarus focused on a case study of the Phoenix metropolitan region in Arizona. Phoenix is an ideal research region as it is located in the hot and arid Sonoran Desert (Hondula and Kuras, 2021), has a population of 4.85 million people (as of 2020), and is rapidly expanding (US Census and Bureau, 2022). Metro Phoenix has an average of 175 days a year with a maximum air temperature above 32 °C (90 °F) (Lawrimore et al., 2016). Despite the extreme heat, the city has been one of the fastest-growing metro regions and is projected to reach 8.04 million by 2050 (State of Arizona, 2018). The high temperatures and the large population create many heat-related health issues (Maricopa County Public Health, 2020) In 2021 there were 338 heat-associated deaths in the region (Baker & Berisha, 2022). Understanding heat exposure during outdoor travel for residents in Metro Phoenix is vital.

The case study simulated the trip and heat exposure for a 3.8 million person synthetic population on June 30th, 2017. Maricopa Association of Governments (MAG) provided the ABM model output developed from the 2010 household survey (Vovsha et al., 2011). The ABM models 18.6 million trips in a day, primarily in-vehicle (93.61 %) and a small portion of active outdoor (5.6 % walking and 0.79 % biking trips). The simulation assumed the population and travel pattern would remain the same in 2017. The ABM included people's daily activities, such as staying home, working, and shopping. Icarus assumed home-based activities happened at the household location, and non-home-based activities happened at non-residential sites, such as offices and shopping malls. The 2018 Maricopa County assessor database (Maricopa County Assessor's Office, 2018) was used to estimate activity locations. For the house locations where the home-based activities took place, Icarus randomly assigned distinct residential parcels to different households. Icarus allocated non-home-based activities to non-residential parcels based on the event descriptions in the ABM. For instance, if the activity purpose was grocery, Icarus assigned commercial parcel locations in the MAZ to those events. Appendix A details the activity

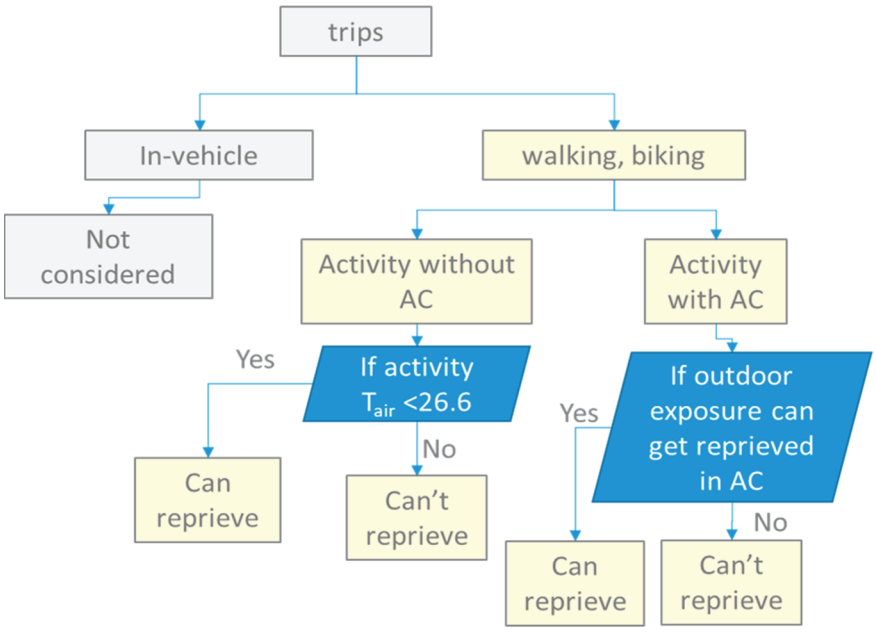

Fig. 2. Decision Tree for Trips Heat Reprieve Assessment.

types and corresponding assigned parcel category. The simulation used the selected parcels for each activity as trip O/D.

Icarus uses the Maricopa County assessor database to estimate AC presence at activity locations. The assessor database details the AC information for residential parcels, and Icarus uses this information to assess the home-based activities heat exposure. For non-residential properties with missing AC details, it was assumed that the following parcel categories did not have AC: barns, farm storages, garages, car wash, and pavilions. Details of the non-residential parcel types and AC assumptions are listed in Appendix B.

The simulation day was hot, with the hottest T_{air} between 28.8 and 43.2 °C (83.9 to 109.7 °F) around 15:00 and the lowest T_{air} between 13.3 and 25.3 °C (55.9 to 77.5 °F) before sunrise (Oak Ridge National Laboratory, 2020). The T_{air} was validated in Thornton et al., 2021. The mean absolute error (MAE) of $T_{air\text{-}max}$ was between 1.21 and 1.34℃ and $T_{air\text{-}min}$ was between 1.07 and 1.2℃ in the case study region (Thornton et al., 2021). 15-minute resolution point-based T_{MRT} was applied (Middel et al., 2017). Middel (et al., 2017) estimated and validated the T_{MRT} along vehicle-accessible roadways by detecting the sky view factors (SVF) of buildings, trees, pavements, and shadings from Google Street View. And the T_{MRT} is calculated using the SVF and an automated radiation model (Middel et al., 2017). T_{MRT} provided temperature after sunrise and before sunset. Since the T_{MRT} readings represent environmental radiance, especially the sun's radiance flux for outdoor environments, it is safe to assume the T_{MRT} is equal to T_{air} before sunrise and after sunset, or in indoor environments (Kántor & Unger, 2011). T_{WBGT} was estimated at street level using the average wind speed in June observed at Phoenix Sky Harbor station, 3.2 m/s (7mph) (Lawrimore et al., 2016), and relative humidity (RH) of 20 %, considering the monsoon season humidity in Phoenix.

3. Results

The results show heat exposure of individuals, heat stress by demographic groups, and explicit locations with high heat stress. A summary of the Icarus simulation results—including the travel speed, trip duration, and distance—is discussed. Heat exposure in T_{air}, T_{MRT}, and T_{WBGT}, and heat stress classifications across different demographic groups are demonstrated. Lastly, locations where travelers are likely to experience excessive heat exposure are discussed.

3.1. Non-motorized trips travel patterns and Icarus simulation statistics

The 3.8 million agents carry out 1.17 million active trips, and Icarus successfully simulated 96 % of those trips. The 4 % of trips not simulated was because the origin and destination of the trip were the same or Icarus could not find a suitable route in the network. Agents from several months old to 93 all have active trips. Excessive heat and pollution exposure produce elevated risks for the very young and senior population (Glass et al., 2015; Hodges et al., 2018). The very young, such as the school-age population or seniors, often travel with at least one other member in the household in the ABM. The simulation captured the group travel behavior described in the ABM by parsing those trips with the exact O/D and trip start and end time. However, these grouped travels are considered as separate trips when analyzing travel and personal heat exposure.

The active trips were short in duration and distance (Table 3). The medium walking and biking trip distances were 1.6 km (1 mile) and 2.8 km (1.7 miles), respectively. Moreover, half of the population spent less than 10.8 min on walking and 8.4 min on biking trips, considering the ingress/egress time. The 90-percentile travel speed was 14.9 kph (9.3 mph) for walking and 38.5 kph (23.9 mph) for biking trips. Although active trips are of short durations in general, certain age groups tend to spend longer on their trips compared to other groups. Around 35 % of the trips by young kids (0 to 5 years) and 26 % by people aged 50 to 65 were over 20 min. Meanwhile, people over 65 spent less time on outdoor travel, as under 4 % of their active trips were over 20 min. The differences in trip duration would impact the heat stress identification when using the heat stress index that considers the event duration, such as the W/R table.

T_{air}, T_{MRT}, and T_{WBGT} reveal different environmental properties and should be assessed independently. As shown in Fig. 3, T_{WBGT} had the lowest temperature range and T_{MRT} had the highest temperature range. The three temperature measures reached their maximum at different times of the day. While the highest T_{MRT} happened around noon when the sun radiance reached its maximum, the hottest T_{air} and T_{WBGT} happened around 15:00. In the ABM, people aged 5 to 20 frequently traveled outside around 15:00 under the hottest T_{air} and T_{WBGT}, while people older than 20 had more active trips around noon with the highest T_{MRT}.

Table 3
Statistics of Icarus simulation results.

	Number of trips[1]	Trip Duration[1] (minutes) *medium (10 %, 90 %)*	**Trip Distance**[2] (km) *medium (10 %, 90 %)*	**Speed**[2] (kph) *medium* (10 %, 90 %)
walking	1,030,014	10.8 (5.9, 25.8) max 72	1.6 (0.6, 3.1)	7.3 (3.2, 14.9)
biking	147,142	8.4 (2.1, 18) max 41	2.8 (0.9, 6)	19 (12.8, 38.5)
car driving	17,245,967	9.1 (2.4, 25.5) max 345	N/A	N/A
public transit	142,869	74.8 (28.7, 131.8) max 208	N/A	N/A

[1] From the ABM output. The trip duration includes ingress/egress waiting time.
[2] From Icarus output.

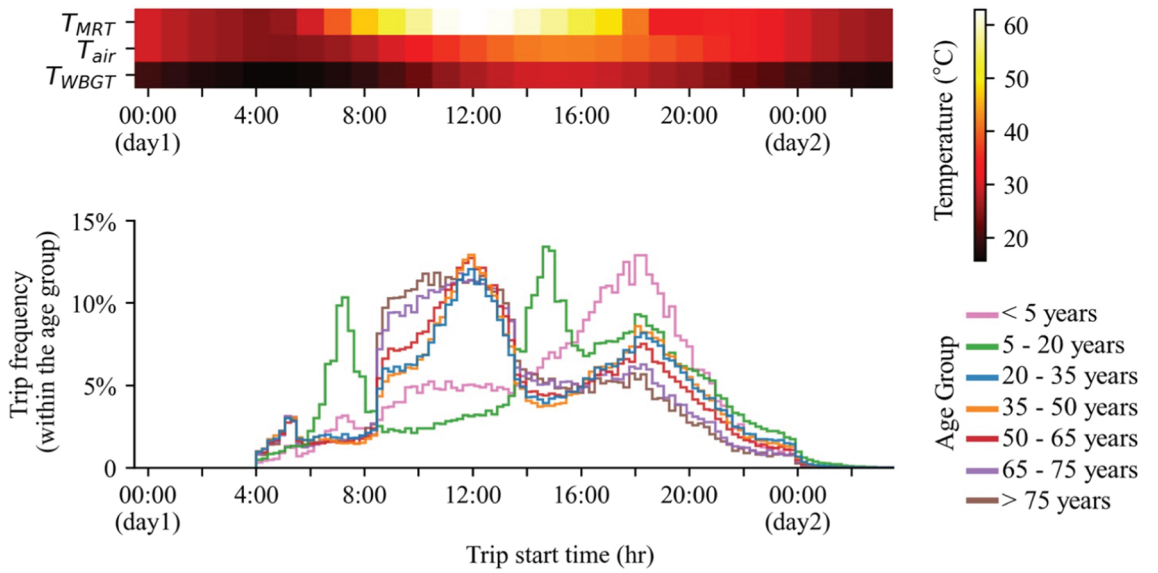

Fig. 3. The Temperature Range (Top) and Trip Frequency for Each Age Group (Bottom) in the Simulation Day.

3.2. Personal heat exposure

Personal heat exposure during outdoor travel varies based on T_{air}, T_{MRT}, and T_{WBGT} measures. The trips had simulated T_{MRT} between 22 and 65 °C (72 to 149°F), T_{air} between 22 and 43 °C (72 to 110°F), and T_{WBGT} between 14 and 31 °C (57 to 87°F). The three temperature measurements provide different framings when assessing heat-vulnerable trips.

3.2.1. Heat stress levels across different age groups

The temperature profiles of T_{air} and T_{MRT} affected the trip exposure estimation considerably wherein the proportion of trips under very hot temperatures significantly shifted within each age group (Fig. 4). The very hot trips, marked as red bars in Fig. 4, were the 25 % of trips with the highest T_{air} or T_{MRT}. People under 20 years had over 35 % of their trips classified as very hot using T_{air}. The same population group would only have 13 % of trips ranked very hot using T_{MRT}. For people between 5 and 20 years old, the ratio of very hot trips under T_{MRT} was 13 %, much lower than the 37 % very hot trips calculated using T_{air}. For the senior population, using T_{MRT} identified more very hot trips compared to T_{air} . For instance for people aged 75+, about 35 % of their active trips were very hot under T_{MRT}. The same age group had fewer very hot trips (about 22 %) under T_{air}. The mismatching of the hottest time of the day in T_{air} and T_{MRT} and the difference in travel behavior (Fig. 3) caused the discrepancy of very hot trips shown in Fig. 4.

Unlike T_{air} and T_{MRT} heat stress classified by T_{WBGT} considered not only the temperature but also the humidity, radiation, wind, and intensity of the travel mode and trip duration. Comparing heat stress using T_{WBGT}, 42 % of trips had no risk since their T_{WBGT} was under 26 °C (Fig. 4). 29.5 % of walking and biking trips were simulated to experience T_{WBGT} between 26 °C and 29 °C, a low

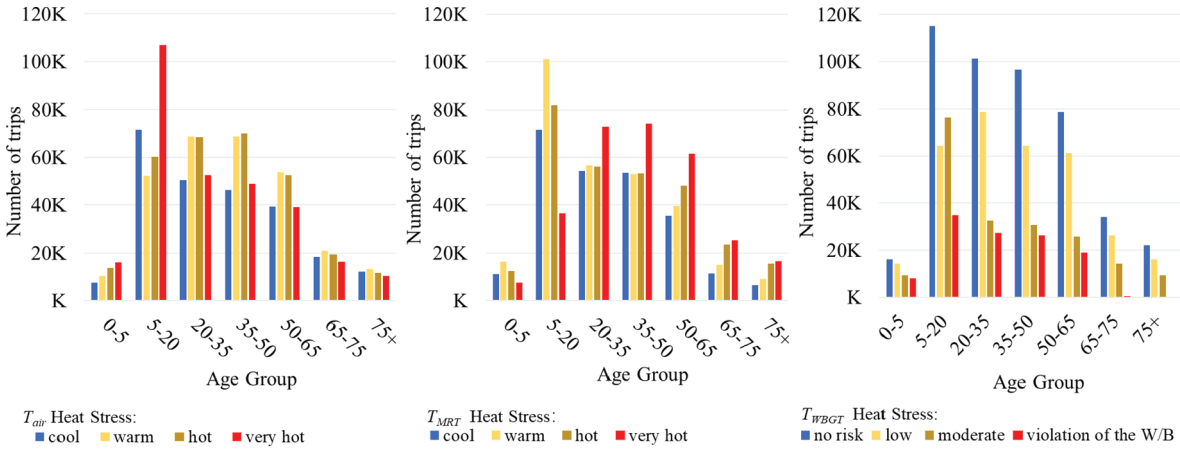

Fig. 4. Trips Heat Stress Level by Age Groups under T_{air}, T_{MRT}, and T_{WBGT}.

risk according to Table 2, and 22.8 % had a moderate risk. However, 10.5 % of active trips violated work/rest cycles in Table 2, although active trips had short durations in general. When considering demographics, a higher ratio (16.9 %) of toddlers (younger than 5) had trips that violate the W/R table. The ratio of trips from senior populations (older than 65) that violated the WBGT W/R table was low (less than 0.3 %), mainly because this demographic group has short-duration trips.

The identified heat-vulnerable trips and population (red bins in Fig. 4) demonstrated distinct patterns when ranking heat stress by the quartiles of T_{air} and T_{MRT}, and the WBGT W/R table. Using T_{WBGT} most (71 %) of trips were identified with no or low risk. Young kids were the most vulnerable while seniors were the least risky when identifying heat stress using T_{WBGT}. 16.9 % of people under 5 had their outdoor trip T_{WBGT} violating Table 2. Meanwhile, less than 0.2 % of trips by people over 75 violated the WBGT W/R table. Using T_{air}, people under 20 were the riskiest as 36 % of their trips were very hot, while the rest of the population had 21 % of their active trips identified as very hot. People over 50 were identified as the most vulnerable using T_{MRT}, as 34 % of their trips had very hot T_{MRT}. Meanwhile, people under 20, the riskiest group identified with T_{air}, had 13 % of their trips under very hot T_{MRT} - the least vulnerable across the population. The heat stress levels identified with T_{MRT} matched with the reports that people aged 75 + had more very high-level heat stress than other population groups (Maricopa County Public Health, 2017, 2020).

3.2.2. Locations with high heat exposure

Most of the city's roadways had few trips in the simulation. Walking and biking travelers used a total length of 3,689 km network. 75 % of roadways had at most 58 trips per day. Only 5 % (184 km) of the network had more than 240 trips passing through. The busiest links in the Phoenix metro region accommodated up to 7,657 trips per day in the simulation. The top 2 % (74 km) most traveled links had a flow of 404 trips per day and were clustered around shopping malls, business centers, city parks, and medical centers (e.g., Carl T Hayden Veterans Affairs Medical Center, Banner Estrella Medical Center).

Although some less traveled corridors had a 100 % *Flow Ratio*, the busiest 5 % corridors had a lower *Flow Ratio* (Table 4). The 100 % *Flow Ratio*, which meant all trips crossing the link were under the top heat stress level, were only identified on corridors with less than 58 trips per day. Cooling strategies implemented on the busiest corridors would benefit more travelers. Therefore, finding links with both large traffic (over 240 trips per day) and a high *Flow Ratio* (over 50 %) are more critical than identifying corridors with little usage but a 100 % *Flow Ratio*. The upper bound *Flow Ratio* for the busiest 5 % links under T_{air} was lower than the corresponding value under T_{MRT} and T_{WBGT}. The *Flow Ratio* under T_{MRT} identified some busiest links that had 63 % to 68 % of their traffic flow from *very hot* trips. Similarly, the *Flow Ratio* under T_{WBGT} shows that the busiest links could have 51 % of trips crossing them violate the W/R table. However, none of the busiest links had a high *Flow Ratio* under T_{air}.

Only the 5 % busiest traveled links were shown to reduce the noise from less travel links but with high *Flow Ratio*. The locations with a high Flow Ratio (over 50 %) under T_{air} and T_{WBGT} were concentrated near downtown Phoenix and major arterials (Fig. 5.b and c). On the contrary, the majority of links had a moderate Flow Ratio between 20 % and 40 % under T_{air} and were evenly distributed across the network (Fig. 5.a).

The Flow Ratio maps demonstrate the locations where very high heat stress trips are likely to occur and create opportunities for planners to design heat mitigation strategies within the network. The disparity of Flow Ratio maps from different temperature measures poses challenges for decision-makers to make investments. Both T_{MRT} and T_{WBGT} consider the heat radiation from the built environment, and locations with a high *Flow Ratio* in Fig. 5.b and c were identified with large low-rise buildings and wide pavements in previous local climate zone studies (Wang et al., 2018). However, different trips purposes and start times, as well as the trip durations, all affect traveler's heat stress and the distribution of *Flow Ratio*. Understanding the reasons behind the disparity of *Flow Ratios* is out of the scope of this study but is a part of ongoing work.

3.3. Trips cannot reprieve during the activity

Travelers who experience heat exposure may get a reprieve from AC during activities. Maricopa county, where the Metro Phoenix is located, has 1.56 million parcels, with one-fifth being non-residential (Fig. 6). 99.8 % of residential parcels have centralized AC or window cooling systems (Maricopa County Assessor's Office, 2018) About 35 % of the non-residential parcels in the County had no climate control measures. It was assumed that garages, warehouses, golf courses, storage facilities, greenhouses, farms, carwashes, barns, and pavilions do not have AC. In the 1.13 million simulated active trips, 72.6 % could reprieve from the excessive heat exposure as the agents destine in an AC-cooled parcel and stay at the parcel long enough. 21.15 % of the active trips ended up on an AC-cooled parcel, but the duration of the activity was too short for these agents to reprieve from the excessive heat exposure. 5.79 % of trips stopped at a parcel with no AC and could not reprieve. Lastly, 0.46 % of trips ended on a no AC-cooled parcel, but both the trips and

Table 4
Flow ratio under different link flow range.

Link Flow Range	Flow Ratio (medium, 1 %, 99 %)		
	T_{air}	T_{MRT}	T_{WBGT}
404 to 7657	23 % (7 %, 39 %)	30 % (14 %, 63 %)	14 % (0 %, **5**1 %)
240 to 403	25 % (10 %, 46 %)	28 % (13 %, 68 %)	15 % (0 %, 51 %)
58 to 239	26 % (7 %, 52 %)	24 % (7 %, 69 %)	16 % (1 %, 23 %)
1 to 57	30 % (5 %, 100 %)	25 % (0 %, 100 %)	24 % (2 %, 100 %)
All (1 to 7657)	28 % (6 %-100 %)	25 % (0–100 %)	20 % (1 %, 100 %)

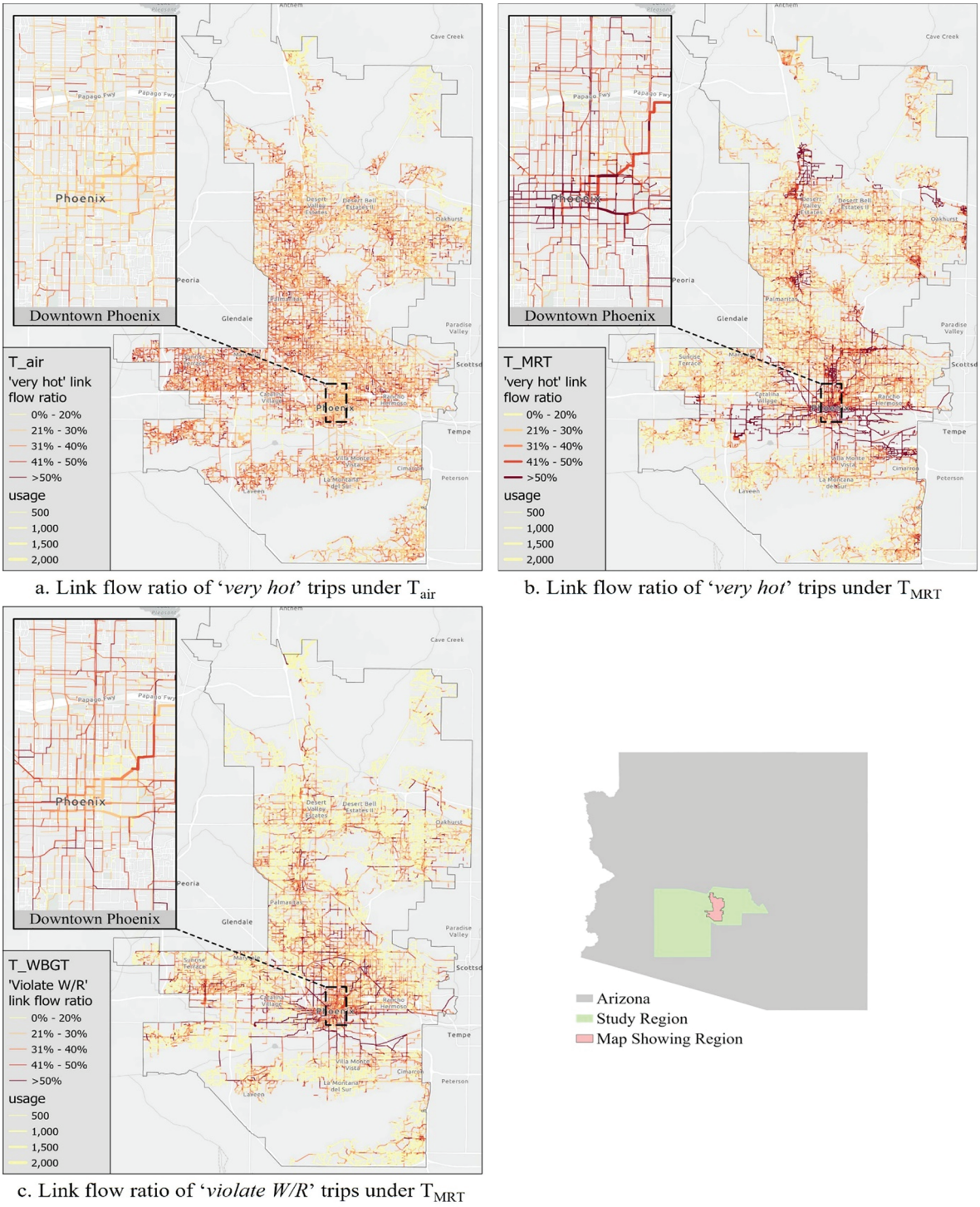

a. Link flow ratio of '*very hot*' trips under T_{air}

b. Link flow ratio of '*very hot*' trips under T_{MRT}

c. Link flow ratio of '*violate W/R*' trips under T_{MRT}

Fig. 5. High Heat exposure Trips Link Flow Ratio under Different Temperatures.

activities happen when T_{air} is below 26.6 °C.

4. Conclusion and discussion

Transportation policies are evolving to meet sustainability goals, emphasizing shifts of travelers away from automobiles to more

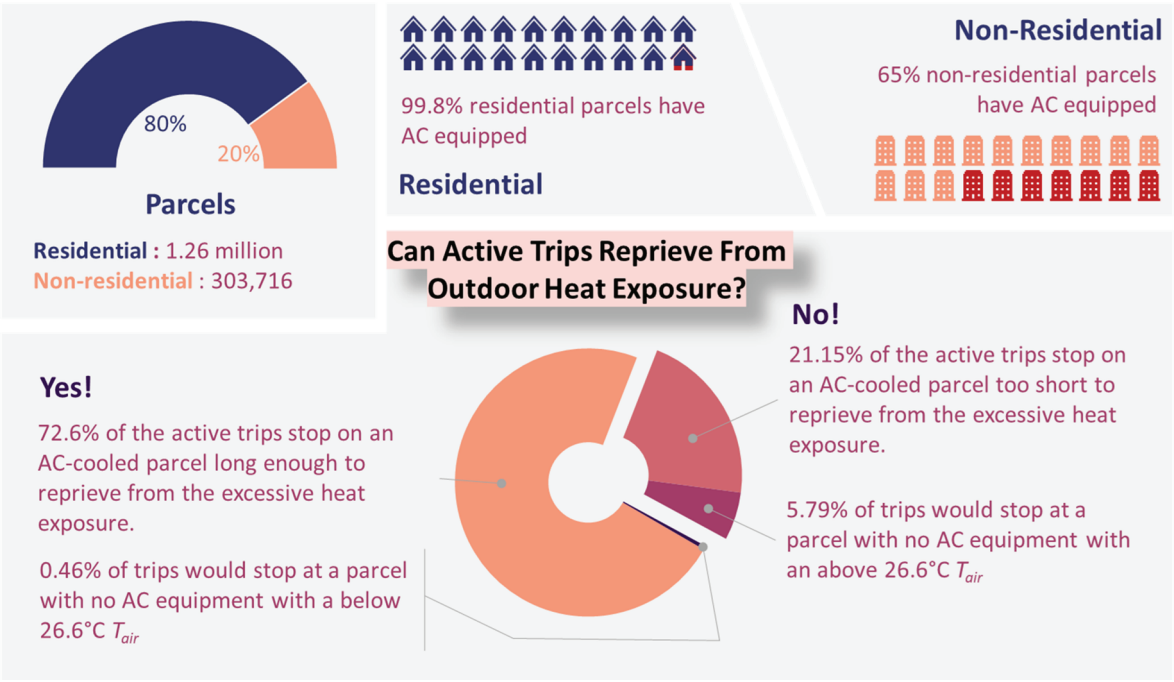

Fig. 6. Infographic of Parcel, AC, and Trips Heat Reprieve.

walking and biking to reduce the emission of greenhouse gasses and air pollutants. The Phoenix metro area has historically been heavily car-dependent, and there is a significant potential to incentivize residents of the region to shift to active trips (Kimball et al., 2013). However, the extreme summer temperatures may limit people's willingness to shift their transportation mode. This study demonstrates a way to understand the personal heat exposure of urban dwellers and to identify the location where high heat exposure travels are likely to occur. This research contributes to the growing studies of personal heat exposure and provides a flexible framework—Icarus—to simulate personal heat exposure at the population scale.

4.1. *Differences in personal heat exposure are revealed with multiple temperature metrics*

Different temperature measures resulted in varying estimates of personal heat exposure. On a population scale, using T_{MRT} to calculate heat exposure, trips that happen around noon are more likely to experience the hottest temperature, while using T_{air} - and T_{WBGT}, the hottest trips are more likely to happen around early afternoon. On a personal scale, people ages 65+ are more likely to experience very hot temperatures under T_{MRT}. In contrast, people younger than 20 are more likely to have very hot heat exposure under T_{air}. With T_{WBGT}, most of the population is classified as under moderate heat risk, and nearly all trips taken by senior residents were classified as safe. At the city scale, the locations where the high heat exposure trips are more likely to happen near city centers and major arterials under T_{MRT} and T_{WBGT}. However, high heat exposure trips under T_{air} are identified near suburban areas. The inconsistency of heat exposure using the different temperature measurements raises the need for further studies to validate the temperature assessments and identify the most appropriate temperature metric for simulations.

4.2. *Novelty of Icarus*

Icarus is the first identified model to combine meteorological data on multiple scales with a transportation network into one platform to simulate personal heat exposure. On the one hand, Icarus is designed to take the ABM of the Phoenix metro for population-scale heat exposure estimation. On the other hand, the modularized design of Icarus allows future users to change the input data based on the specific study region or focus on the personal heat exposure simulation. Icarus also efficiently utilizes computational resources and manages voluminous data, especially for large-scale analysis. For instance, it takes 30 min to simulate the personal heat exposure of 3.8 million agents with 1.17 million active trips in the Phoenix metropolitan Area. The rich information in the Icarus output opens opportunities for studying the population-scale heat risk and infrastructure planning that affect heat exposure. Icarus differs from previous personal heat exposure simulation models that considered human thermal response to heat (Glass et al., 2015) but did not consider travel and activity behavior. However, future updates can incorporate the human heat balance model into Icarus to help identify heat stress.

4.3. Limitations

Icarus's limitations come from simplifying the travel model and different temperature metrics. Uncertainties were introduced into the model during the random selection of parcels in the MAZ and assuming the shortest path as the routes agents would choose. Traveler walking or biking path choice could be affected by safety, preference, or street perceptions and conditions (Marshall & Garrick, 2010; Titze et al., 2012). Different temperature metrics complicate the result interpretation, as the high heat stress population and locations depend on the metric used for analysis. Previous studies pointed out that T_{air} is not a comprehensive indicator of personal heat exposure as it is only one of the several environmental factors (Hondula and Kuras, 2021; Kuras et al., 2017). While the T_{WBGT} is widely used to identify the heat stress risk, the WBGT W/B table has its limitations in identifying the heat stress for the senior population. More research must be done to identify the temperature metrics most suitable for personal heat exposure study. While most trips were simulated with reasonable travel speed, about 10 % of the active trips had unrealistic fast velocities. The uncertainty of the travel speed came from three aspects: either the trip duration provided by the ABM could be too short, the O/D provided in ABM was too long, or Icarus assigned activities in parcels away. However, checking the accuracy of the ABM data and providing accurate downscale strategies to extract location from the MAZ level to the parcel level is outside this study's scope. Besides, urban heat itself is driven by wasted heat from building, high coverage of pavement, parking lots, and vehicles. While T_{MRT} addressed the wasted heat from building and impervious surfaces, the heat emission from vehicles was not considered in this study.

Despite the limitations Icarus creates significant advances in person-based heat exposure assessment. The module provides a more detailed look at exposure to extreme heat by using ABMs to create a bottom-up picture of heat exposure at a population scale. Incorporating high-resolution spatiotemporal temperature enhances the proxy variables, such as land surface air temperature used in previous studies. Considering the heat exposure along the transportation network, Icarus spotlights the effect of the built environment and travel behavior on personal heat exposure. Icarus could enhance our understanding of the relationship between exposure to extreme heat and social vulnerability and their role in influencing heat risk.

CRediT authorship contribution statement

Rui Li: Conceptualization, Methodology, Writing – original draft, Writing – review & editing. **Mikhail V. Chester:** Conceptualization, Methodology, Writing – review & editing. **David M. Hondula:** Conceptualization, Methodology, Writing – review & editing. **Ariane Middel:** Conceptualization, Methodology, Writing – review & editing. **Jennifer K. Vanos:** Methodology, Writing – review & editing. **Lance Watkins:** Writing – review & editing.

Declaration of Competing Interest

The authors declare that they have no known competing financial interests or personal relationships that could have appeared to influence the work reported in this paper.

Acknowledgments

We would like to express our gratitude to MAG for providing the ABM data, and to Ben Brownlee of ASU for initializing the Icarus program. Map data copyrighted by OpenStreetMap contributors and available from https://www.openstreetmap.org. This study was funded by United States National Science Foundation award CMMI-1635490 (A Simulation Platform to Enhance Infrastructure and Community Resilience to Extreme Heat Events), and CMMI-1942805 (CAREER: Human Thermal Exposure in Cities - Novel Sensing and Modeling to Build Heat-Resilience).

References

ACGIH, 2019. TLVs and BEIs: Based on the documentation of the threshold limit values for chemical substances and physical agents & biological exposure indices. ACGIH.

Aminipouri, M., Knudby, A.J., Krayenhoff, E.S., Zickfeld, K., Middel, A., 2019. Modelling the impact of increased street tree cover on mean radiant temperature across Vancouver's local climate zones. Urban For. Urban Green. 39 (July 2018), 9–17. https://doi.org/10.1016/j.ufug.2019.01.016.

Baker, T., & Berisha, V. (2022). 2021 Heat Deaths. Maricopa County Department of Public Health. https://www.maricopa.gov/DocumentCenter/View/74257/Final-2021-Heat-Deaths#:~:text=338%20heat%2Dassociated%20deaths%20were,a%2069.8%25%20increase%20from%202019.&text=The%20proportion%20of%20indoor%20heat,2018%20but%20increased%20for%202021.

Bao, J., Li, X., Yu, C., 2015. The Construction and Validation of the Heat Vulnerability Index, a Review. Int. J. Environ. Res. Public Health 12 (7), 7220–7234. https://doi.org/10.3390/ijerph120707220.

Bernhard, M.C., Kent, S.T., Sloan, M.E., Evans, M.B., McClure, L.A., Gohlke, J.M., 2015. Measuring personal heat exposure in an urban and rural environment. Environ. Res. 137, 410–418. https://doi.org/10.1016/j.envres.2014.11.002.

Budd, G.M., 2008. Wet-bulb globe temperature (WBGT)—Its history and its limitations. J. Sci. Med. Sport 11 (1), 20–32. https://doi.org/10.1016/j.jsams.2007.07.003.

Chow, W.T.L., Chuang, W.-C., Gober, P., 2012. Vulnerability to extreme heat in metropolitan phoenix: spatial, temporal, and demographic dimensions. Prof. Geogr. 64 (2), 286–302. https://doi.org/10.1080/00330124.2011.600225.

City of Mesa. (2014). Mesa 2040 General Plan. City of Mesa. https://www.mesaaz.gov/home/showdocument?id=12298.

de Nazelle, A., Morton, B.J., Jerrett, M., Crawford-Brown, D., 2010. Short trips: an opportunity for reducing mobile-source emissions? Transp. Res. Part D: Transp. Environ. 15 (8), 451–457. https://doi.org/10.1016/j.trd.2010.04.012.

Eisenman, D.P., Wilhalme, H., Tseng, C.-H., Chester, M., English, P., Pincetl, S., Fraser, A., Vangala, S., Dhaliwal, S.K., 2016. Heat Death Associations with the built environment, social vulnerability and their interactions with rising temperature. Health Place 41, 89–99. https://doi.org/10.1016/j.healthplace.2016.08.007.

Epstein, Y., Moran, D.S., 2006. Thermal Comfort and the Heat Stress Indices. Ind. Health 44 (3), 388–398. https://doi.org/10.2486/indhealth.44.388.

FlLOW Project, 2016. The Role of Walking and Cycling in Reducing Congestion: A Porfolio of Measures. http://www.h2020-flow.eu.
Glass, K., Tait, P.W., Hanna, E.G., Dear, K., 2015. Estimating risks of heat strain by age and sex: a population-level simulation model. Int. J. Environ. Res. Public Health 12 (5), Article 5. https://doi.org/10.3390/ijerph120505241.
Hagberg, A.A., Schult, D.A., Swart, P.J., 2008. Exploring network structure. Dyn. Function NetworkX. 11–16.
Hamer, M., Chida, Y., 2008. Active commuting and cardiovascular risk: a meta-analytic review. Prev. Med. 46 (1), 9–13. https://doi.org/10.1016/j.ypmed.2007.03.006.
Health, M.C.P., 2017. Heat-Associated Death in Maricopa County. Maricopa County Public Health, AZ.
Hodges, G.J., Kiviniemi, A.M., Mallette, M.M., Klentrou, P., Falk, B., Cheung, S.S., 2018. Effect of passive heat exposure on cardiac autonomic function in healthy children. Eur. J. Appl. Physiol. 118 (10), 2233–2240. https://doi.org/10.1007/s00421-018-3957-1.
Hoehne, C.G., Chester, M.V., Sailor, D.J., King, D.A., 2020. Urban heat implications from parking, roads, and cars: a case study of metro phoenix. Sustain. Resilient Infrastruct. 7 (4), 272–290.
Hondula, D.M., Davis, R., 2012. P-414: The characteristics of places within seven U.S. cities where the mortality rate is highest during extreme heat events. Epidemiology 23 (5S). https://doi.org/10.1097/01.ede.0000417413.00991.f9.
Hondula, D.M., Georgescu, M., Balling, R.C., 2014. Challenges associated with projecting urbanization-induced heat-related mortality. Sci. Total Environ. 490, 538–544. https://doi.org/10.1016/j.scitotenv.2014.04.130.
Hondula, D.M., Kuras, E.R., 2021. Novel metrics for relating personal heat exposure to social risk factors and outdoor ambient temperature. Environment International 146. https://doi.org/10.1016/j.envint.2020.106271.
Hondula, D.M., Kuras, E.R., Betzel, S., Drake, L., Eneboe, J., Kaml, M., Munoz, M., Sevig, M., Singh, M., Ruddell, B.L., Harlan, S.L., 2021. Novel metrics for relating personal heat exposure to social risk factors and outdoor ambient temperature. Environ. Int. 146, 106271.
Iverson, S.A., Gettel, A., Bezold, C.P., Goodin, K., McKinney, B., Sunenshine, R., Berisha, V., 2020. Heat-associated mortality in a hot climate: Maricopa County, Arizona, 2006–2016. Public Health Rep. 135 (5), 631–639. https://doi.org/10.1177/0033354920938006.
Kamruzzaman, M.d., Deilami, K., Yigitcanlar, T., 2018. Investigating the urban heat island effect of transit oriented development in Brisbane. J. Transp. Geogr. 66, 116–124. https://doi.org/10.1016/j.jtrangeo.2017.11.016.
Kántor, N., Unger, J., 2011. The most problematic variable in the course of human-biometeorological comfort assessment—The mean radiant temperature. Open Geosci. 3 (1), 90–100. https://doi.org/10.2478/s13533-011-0010-x.
Karner, A., Hondula, D.M., Vanos, J.K., 2015. Heat exposure during non-motorized travel: Implications for transportation policy under climate change. J. Transp. Health 2 (4), 451–459. https://doi.org/10.1016/j.jth.2015.10.001.
Kimball, M., Chester, M., Gino, C., Reyna, J., 2013. Assessing the potential for reducing life-cycle environmental impacts through transit-oriented development infill along existing light rail in phoenix. J. Plan. Educ. Res. 33 (4), 395–410. https://doi.org/10.1177/0739456X13507485.
Kolbe, K., 2019. Mitigating urban heat island effect and carbon dioxide emissions through different mobility concepts: comparison of conventional vehicles with electric vehicles, hydrogen vehicles and public transportation. Transp. Policy 80, 1–11. https://doi.org/10.1016/j.tranpol.2019.05.007.
Kuras, E. R., Richardson, M. B., Calkins, M. M., Ebi, K. L., Hess, J. J., Kintziger, K. W., Jagger, M. A., Middel, A., Scott, A. A., Spector, J. T., Uejio, C. K., Vanos, J. K., Zaitchik, B. F., Gohlke, J. M., & Hondula, D. M. (2017). Opportunities and challenges for personal heat exposure research. Environ. Health Perspect. 125(8). Doi: 10.1289/EHP556.
Kuras, E.R., Hondula, D.M., Brown-Saracino, J., 2015. Heterogeneity in individually experienced temperatures (IETs) within an urban neighborhood: Insights from a new approach to measuring heat exposure. Int. J. Biometeorol. 59 (10), 1363–1372. https://doi.org/10.1007/s00484-014-0946-x.
Lawrimore, J., Ray, R., Applequist, S., Korzeniewski, B., Menne, M.J., 2016. Global Summary of the Month (GSOM), Version 1. NOAA National Centers for Environmental Information.
Maricopa County Assessor's Office. (2018). Maricopa County Parcel Data. https://maps.mcassessor.maricopa.gov/.
Maricopa County Public Health. (2020). Heat-Associated Death in Maricopa County, AZ (p. 73). Maricopa County Public Health.
Marshall, W.E., Garrick, N.W., 2010. Effect of street network design on walking and biking. Transp. Res. Rec. 2198 (1), 103–115. https://doi.org/10.3141/2198-12.
Middel, A., Lukasczyk, J., Maciejewski, R., 2017. Sky view factors from synthetic fisheye photos for thermal comfort routing—a case study in phoenix, Arizona. Urban Planning 2 (1), 19–30. https://doi.org/10.17645/up.v2i1.855.
National Cancer Institute. (2002). Metabolic Equivalent of Task Values for Activities in American Time Use Survey and 2002 Census Occupational Classification System. https://epi.grants.cancer.gov/physical/met/atus-met.php?major[ ]=17&keywords=&metval_min=&metval_max=.
Oak Ridge National Laboratory. (2020). Daymet. Daymet. https://daymet.ornl.gov/.
OpenStreetMap Contributors. (2015). OpenStreetMap. OpenStreetMap. https://www.openstreetmap.org/.
OSHA. (2015). OSHA Technical Manual (OTM)—Section III: Chapter 4 | Occupational Safety and Health Administration. https://www.osha.gov/otm/section-3-health-hazards/chapter-4.
Pendyala, R.M., Kitamura, R., Chen, C., Pas, E.I., 1997. An activity-based microsimulation analysis of transportation control measures. Transp. Policy 4 (3), 183–192. https://doi.org/10.1016/S0967-070X(97)00005-X.
Phoenix, 2021. Climate Action Plan. City of Phoenix.
Pörtner, H.-O., Roberts, D. C., Tignor, M. M. B., Poloczanska, E. S., Mintenbeck, K., Alegría, A., Craig, M., Langsdorf, S., Löschke, S., Möller, V., Okem, A., & Rama, B. (Eds.), 2022. Summary for policymakers. In Climate Change 2022: Impacts, Adaptation and Vulnerability. Contribution of Working Group II to the Sixth Assessment Report of the Intergovernmental Panel on Climate Change. Cambridge University Press.
Reid, C.E., O'Neill, M.S., Gronlund, C.J., Brines, S.J., Brown, D.G., Diez-Roux, A.V., Schwartz, J., 2009. Mapping community determinants of heat vulnerability. Environ. Health Perspect. 117 (11), 1730–1736.
State of Arizona, 2018. Arizona State and County Population Projections, 2018-2055: Methodology Report (p. 31). https://www.azcommerce.com/media/1544715/pop-prj-state-county-2018methodology.pdf.
Stull, R., 2011. Wet-bulb temperature from relative humidity and air temperature. J. Appl. Meteorol. Climatol. 50 (11), 2267–2269. https://doi.org/10.1175/JAMC-D-11-0143.1.
Sutherland, A., 2015. Wet Bulb Globe Temperature: What It Is and How To Use It | Weather and Agriculture: A Plains Perspective. http://blog.mesonet.org/agriculture/wet-bulb-globe-temperature-what-it-is-and-how-to-use-it/.
Thornton, P.E., Shrestha, R., Thornton, M., Kao, S.-C., Wei, Y., Wilson, B.E., 2021. Gridded daily weather data for North America with comprehensive uncertainty quantification. Sci. Data 8 (1), Article 1. https://doi.org/10.1038/s41597-021-00973-0.
Titze, S., Krenn, P., Oja, P., 2012. Developing a bikeability index to score the biking-friendliness of urban environments. J. Sci. Med. Sport 15, S29–S30. https://doi.org/10.1016/j.jsams.2012.11.071.
Tudor-Locke, C., Johnson, W.D., Katzmarzyk, P.T., 2009. Accelerometer-determined steps per day in US adults. Med. Sci. Sports Exerc. 41 (7), 1384–1391. https://doi.org/10.1249/MSS.0b013e318199885c.
US Census Bureau. (2022, January 24). 2020 Census. Census.Gov. https://www.census.gov/2020census.
Vanos, J.K., Rykaczewski, K., Middel, A., Vecellio, D.J., Brown, R.D., Gillespie, T.J., 2021. Improved methods for estimating mean radiant temperature in hot and sunny outdoor settings. Int. J. Biometeorol. 65 (6), 967–983. https://doi.org/10.1007/s00484-021-02131-y.
Vovsha, P., Freedman, J., Livshits, V., Sun, W., 2011. Design features of activity-based models in practice coordinated travel-regional activity modeling platform. Transport. Res. Record: J. Transport. Res. 300, 19–27. https://doi.org/10.3141/2254-03.
Wang, C., Middel, A., Myint, S.W., Kaplan, S., Brazel, A.J., Lukasczyk, J., 2018. Assessing local climate zones in arid cities: the case of Phoenix, Arizona and Las Vegas, Nevada. ISPRS J. Photogramm. Remote Sens. 141, 59–71. https://doi.org/10.1016/j.isprsjprs.2018.04.009.
Yoo, E., Rudra, C., Glasgow, M., Mu, L., 2015. Geospatial estimation of individual exposure to air pollutants: moving from static monitoring to activity-based dynamic exposure assessment. Ann. Assoc. Am. Geogr. 105 (5), 915–926. https://doi.org/10.1080/00045608.2015.1054253.